

Fluctuation relations in non-equilibrium stationary states of Ising models.

A Piscitelli¹, F Corberi², G Gonnella¹ and A Pelizzola³

¹ Dipartimento di Fisica, Università di Bari and Istituto Nazionale di Fisica Nucleare, Sezione di Bari, via Amendola 173, 70126 Bari, Italy

² Dipartimento di Matematica ed Informatica, via Ponte don Melillo, Università di Salerno, 84084 Fisciano (SA), Italy

³Dipartimento di Fisica and Istituto Nazionale di Fisica Nucleare, Sezione di Torino, and CNISM, Politecnico di Torino, c. Duca degli Abruzzi 24, 10129 Torino, Italy

E-mail: piscitelli@ba.infn.it, corberi@sa.infn.it, gonnella@ba.infn.it, alessandro.pelizzola@polito.it

Abstract.

Fluctuation relations for the entropy production in non equilibrium stationary states of Ising models are investigated by Monte Carlo simulations. Systems in contact with heat baths at two different temperatures or subject to external driving will be studied. In the first case, by considering different kinetic rules and couplings with the baths, the behavior of the probability distributions of the heat exchanged in a time τ with the thermostats, both in the disordered and in the low temperature phase, are discussed. The fluctuation relation is always verified in the large τ limit and deviations from linear response theory are observed. Finite- τ corrections are shown to obey a scaling behavior. In the other case the system is in contact with a single heat bath but work is done by shearing it. Also for this system the statistics collected for the mechanical work shows the validity of the fluctuation relation and preasymptotic corrections behave analogously to the case with two baths.

PACS numbers: 05.70.Ln; 05.40.-a; 75.40.Gb

1. Introduction

In equilibrium statistical mechanics the knowledge of general expressions for the probabilities of microscopic configurations is the cornerstone of a successful theory describing the macroscopic behavior of a large variety of physical systems. Similar expressions, however, are not known for systems in non-equilibrium steady states (NESS), despite their widespread occurrence in nature and their practical interest.

NESS are usually realized by driving a system, either mechanically, as in the case of sheared or stirred fluids, or thermodynamically, due for instance to couplings to reservoirs at different temperatures. These states are characterized by a finite rate of entropy production, and the recent proposal [1, 2, 3] of a relation governing the fluctuations of this quantity constitutes an important result of general validity. The relation connects the probability $\mathcal{P}(\Sigma(\tau))$ of producing an entropy $\Sigma(\tau)$ in a time interval τ , with the probability of the opposite quantity, according to

$$\ln \frac{\mathcal{P}(\Sigma(\tau))}{\mathcal{P}(-\Sigma(\tau))} = -\Sigma(\tau). \quad (1)$$

Eq. (1), also known as Gallavotti-Cohen relation, holds in the large τ limit, specifically with τ larger than all relaxation times of the system. It was proved as a theorem for a specific class of dynamical systems in [3] and then established for stochastic kinetics in [4, 5, 6]. Expressions related to Eq. (1) have been established in Refs. [7, 8, 9, 10, 11, 12, 13]. Recent reviews are given in [14].

Fluctuation relations (FRs) are expected to be relevant in mesoscopic systems, particularly in nano- and biological sciences [15], because at these scales typical thermal fluctuations may be sufficiently large to be comparable with the magnitude of the external driving. FRs have nowadays been tested in some experiments [16, 17, 18].

In this work we study the FRs in simple standard statistical models, where their validity can be ascertained, and some of the mechanisms of their occurrence can be investigated. We consider the Ising model as a paradigmatic example of interacting system interested by a phase transition. The model is maintained in NESS either by coupling it to two thermal baths at different temperatures T_1, T_2 , or by a mechanical forcing. In the former case, introducing $\Delta\beta^{(1)} = -\Delta\beta^{(2)} = \left(\frac{1}{T_2} - \frac{1}{T_1}\right)$, the relation (1) can be specified as

$$\ln \frac{\mathcal{P}(Q^{(n)}(\tau))}{\mathcal{P}(-Q^{(n)}(\tau))} = Q^{(n)}(\tau)\Delta\beta^{(n)}, \quad (2)$$

where $Q^{(n)}(\tau)$ is the heat exchanged with the heat bath at temperature T_n ($n = 1, 2$) in a time τ . With mechanical driving Eq. (1) can be cast as

$$\ln \frac{\mathcal{P}(\mathcal{W}(\tau))}{\mathcal{P}(-\mathcal{W}(\tau))} = \frac{\mathcal{W}(\tau)}{T}, \quad (3)$$

where $\mathcal{W}(\tau)$ is the work done on the system in the time interval τ and T is the temperature of the thermostat.

In the case of thermodynamic driving, the relation (2) has been previously studied for different systems. It was shown to hold [19] for a chain of oscillators coupled at the extremities to two thermostats, and it was studied [20] for a Brownian particle in contact with two reservoirs. A fluctuation relation has been proved in [21] for the heat exchanged between two systems initially prepared in equilibrium at different temperatures and later put in contact. The case of the Ising model coupled to different reservoirs, similar to that considered in this paper, has been studied analytically in [22], in a mean-field approximation. Fluctuation properties of work due to a magnetic field in transient regimes of Ising model have been analyzed in [23]. We are not aware of studies of the relation (3) in stationary states of mechanically driven Ising models.

In this Article we show that the FRs hold in the large- τ limit for the nearest neighbour Ising model and both kinds of NESS analyzed. In the case of NESS induced by the presence of two thermostats, we also consider different couplings with the baths and kinetic rules, some of which have been previously reported in [24], in order to address the generality of the results. Our numerical data allow to appreciate and characterize the finite time corrections to the asymptotic result. These were shown to be of order $1/\tau$ in [3, 25, 26]. For systems described by a Langevin equation, in cases corresponding to the experimental setup consisting of a resistor and a capacitor in parallel, finite time corrections also behave as $1/\tau$ when work fluctuations are considered [11, 17], while faster decays have been predicted for other topologies of circuits [11]. Our data show that the leading term of such corrections decays as $1/\tau$. We also propose an expression which well describes the corrections in an extended range of values of τ , incorporating the sub-leading behavior. This expression implies a scaling behavior which takes into account the geometry of the system and the nature of the coupling with the heat baths.

The occurrence of a phase transition in the Ising model allows us to discuss the interplay between the breaking of ergodicity and the validity of the fluctuation relation. A finite size system in the low temperature NESS remains trapped into broken symmetry states for a time τ_{erg} that diverges in the thermodynamic limit, much like in equilibrium. By varying the system size and the baths temperatures, we are able to investigate the large- τ limit both in the regime $\tau \gg \tau_{erg}$ and $\tau \ll \tau_{erg}$. The latter is particularly interesting because in this case, since FRs are expected to hold for τ much larger than the characteristic relaxation times of the systems, they are not necessarily obeyed in this condition. Interestingly, instead, we find that, the FR (2) holds true in any case.

Close to equilibrium the FR implies the Green-Kubo relation (GKR) [27]. Therefore, as discussed in [26] a stringent test of the FR, which cannot be reduced to linear response theory, can be only achieved when the drive is large enough to bring the system far from equilibrium, spoiling the GKR and/or determining non-Gaussian $\mathcal{P}(\mathcal{Q}^{(n)})$. An analysis of the data in the case of thermodynamic driving will allow us to provide a strict test of the validity of the FR also in the far from equilibrium regime.

The paper is organized as follows. In the next section we introduce the model and discuss two different implementations of the coupling to the heat baths. Then the results of our simulations will be presented and interpreted in terms of scaling expressions for

finite time corrections. Relations with linear response theory are discussed in Sect. 2.3. In Section 3 the model with mechanical driving is considered. Section 4 includes our conclusions and a discussion of the perspectives of this work.

2. Systems in contact with heat baths at two temperatures

2.1. The models

We consider a two-dimensional Ising model defined by the Hamiltonian $H\{\sigma\} = -J \sum_{\langle ij \rangle} \sigma_i \sigma_j$, where $\sigma_i = \pm 1$ is a spin variable on a site i of a rectangular lattice with $N = M \times L$ sites, $\{\sigma\}$ is the configuration of all the spins and the sum is over all pairs $\langle ij \rangle$ of nearest neighbors.

In the case of *statical* coupling with the heat baths the system is divided into two halves. The left part (the first $M/2$ vertical lines) interacts with the heat bath at temperature T_1 while the right part is in contact with the reservoir at $T_2 > T_1$. We have implemented both open or periodic boundary conditions. We used Monte Carlo spin-exchange (Kawasaki) dynamics, corresponding to systems with conserved magnetization. The case with single spin dynamics was considered previously [24]. In the present case with two heat baths, we have implemented the Kawasaki rule as follows: picking at random a couple of nearest neighbor spins σ_l, σ_m we attempt their exchange according to standard Metropolis transition rates

$$\mathcal{A}(\{\sigma'\}, \{\sigma\}) = \min \left\{ \exp \left[-\frac{\Delta E(\{\sigma\}, \{\sigma'\})}{T} \right], 1 \right\}, \quad (4)$$

where $\{\sigma\}$ and $\{\sigma'\}$ are the configurations before and after the move and $\Delta E(\{\sigma\}, \{\sigma'\}) = H\{\sigma'\} - H\{\sigma\}$. The temperature T to be entered in $\mathcal{A}(\{\sigma'\}, \{\sigma\})$ is chosen as follows: if both the spins considered are in contact with the same bath, T is the temperature of that thermostat. In the case in which, say, σ_m is coupled to the temperature T_1 and σ_l to T_2 , we compute $\Delta E(\{\sigma\}, \{\sigma'\})/T$ by splitting the two contributions from the different reservoirs, namely $\Delta E(\{\sigma\}, \{\sigma'\})/T = -(J/T_2)\sigma'_l \sum_{\langle i \rangle_l} \sigma'_i - (J/T_1)\sigma'_m \sum_{\langle i \rangle_m} \sigma'_i + (J/T_2)\sigma_l \sum_{\langle i \rangle_l} \sigma_i + (J/T_1)\sigma_m \sum_{\langle i \rangle_m} \sigma_i$, where $\langle i \rangle_l$ ($\langle i \rangle_m$) are nearest neighbors of σ_l (σ_m).

In the second implementation, using single-spin dynamics, each spin σ_i , at a given time t , is put *dynamically* in contact with one or the other reservoir depending on the (time dependent) value of $h_i = (1/2) |\sum_{\langle j \rangle_i} \sigma_j|$, where the sum runs over the nearest neighbor spins σ_j of σ_i . Notice that h_i is one half of the (absolute value) of the local field. In two dimensions, with periodic boundary conditions, the possible values of h_i are $h_i = 0, 1, 2$. At each time, spins with $h_i = 2$ are connected to the bath at $T = T_1$ and those with $h_i = 1$ with the reservoir at $T = T_2$. Namely, when a particular spin σ_i is updated, the temperature T_1 or T_2 is entered into the transition rate according to the value of h_i . Loose spins with $h_i = 0$ can flip back and forth regardless of temperature because these moves do not change the energy of the system. Then, as in the usual Ising model, they are associated to a temperature independent transition rate. Notice that

$h_i = 2$ correspond to spins whose surrounding neighbors are aligned, a situation which is typically found in the bulk of ordered domains, while $h_i = 1$ corresponds to interfacial spins. This model was introduced in [28] and studied in [29]. It is characterized by a line of critical points in the plane T_1, T_2 , separating a ferromagnetic from a paramagnetic phase analogously to the equilibrium Ising model. Metropolis transition rates have been considered also in this case.

Considering the stationary state, a generic evolution of the system is given by the sequence of configurations $\{\sigma(t)\} = \{\sigma_1(t), \dots, \sigma_N(t)\}$ where $\sigma_i(t)$ is the value of the spin variable at time t . Denoting with $t_k^{(n)}$ the times (measured here as the number of elementary Montecarlo updates) at which an elementary move is attempted by coupling the system to the n -th reservoir, the heat released by the bath in a time window $[s, s + \tau]$ is defined as

$$\mathcal{Q}^{(n)}(\tau) = \sum_{\{t_k^{(n)}\} \subset [s, s+\tau]} [H(\sigma(t_k^{(n)})) - H(\sigma(t_k^{(n)} - 1))]. \quad (5)$$

In the case of dynamic coupling to the thermostats, recalling the discussion above, $\mathcal{Q}^{(1)}(\tau)$ and $\mathcal{Q}^{(2)}(\tau)$ will be also referred to as *bulk* and *interface* exchanged heats. The properties of $\mathcal{Q}^{(n)}(\tau)$ will be computed by collecting the statistics over different subtrajectories obtained by dividing a long history of length t_F into many (t_F/τ) time-windows of length τ , starting from different s .

Notice that all the dynamical rules considered insofar obey the generalized detailed balance condition [30]

$$e^{\mathcal{Q}^{(1)}/T_1 + \mathcal{Q}^{(2)}/T_2} \mathcal{A}(\{\sigma'\}, \{\sigma\}) = \mathcal{A}(\{\sigma\}, \{\sigma'\}) \quad (6)$$

where $\mathcal{Q}^{(1)}, \mathcal{Q}^{(2)}$ are the heats exchanged with the reservoirs during an elementary transition.

2.2. Results for $T_1, T_2 > T_c$

We begin our analysis with the study of the relation (2) in the case with both temperatures above the critical value $T_c \simeq 2.269$ of the equilibrium Ising model. In the following we will measure times in montecarlo steps (MCS) (1 MCS=N elementary moves) and set $J = 1$.

The typical behavior of the heat probability distributions (PD) is reported in Fig. 1 for the system with static coupling to the baths, $T_1 = 2.9$, $T_2 = 3$, and a square geometry with $L = M = 20$. Much larger sizes can be hardly used because trajectories with a heat whose sign is opposite to that of the average value would be too rare. Results are qualitatively similar to those obtained with non-conserved dynamics [24]. $\mathcal{Q}^{(1)}(\tau)$ ($\mathcal{Q}^{(2)}(\tau)$) is on average negative (positive) and the relation

$$\langle \mathcal{Q}^{(1)}(\tau) \rangle + \langle \mathcal{Q}^{(2)}(\tau) \rangle = 0 \quad (7)$$

is verified. The PDs for $\mathcal{Q}^{(1)}$ and $\mathcal{Q}^{(2)}$ are similar but when $\Delta T = T_2 - T_1$ is increased the distribution of $\mathcal{Q}^{(1)}$ can be observed to be more peaked.

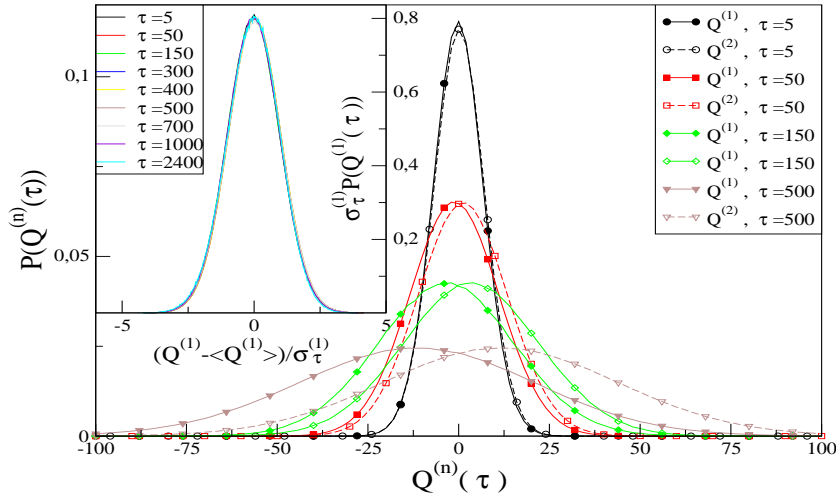


Figure 1. Heat PDs for $Q^{(1)}$ (on the left) and $Q^{(2)}$ (on the right) for a system evolving with spin-exchange-dynamics and $T_1 = 2.9, T_2 = 3$, size 20×20 and $t_F = 5 \cdot 10^8$ MCS. In the inset $\sigma_\tau^{(1)} P(Q^{(1)}(\tau))$ is plotted against $(Q^{(1)}(\tau) - \langle Q^{(1)}(\tau) \rangle) / \sigma_\tau^{(1)}$. Curves for different τ collapse on a Gaussian mastercurve. The same collapse of data would be observed for $Q^{(2)}$.

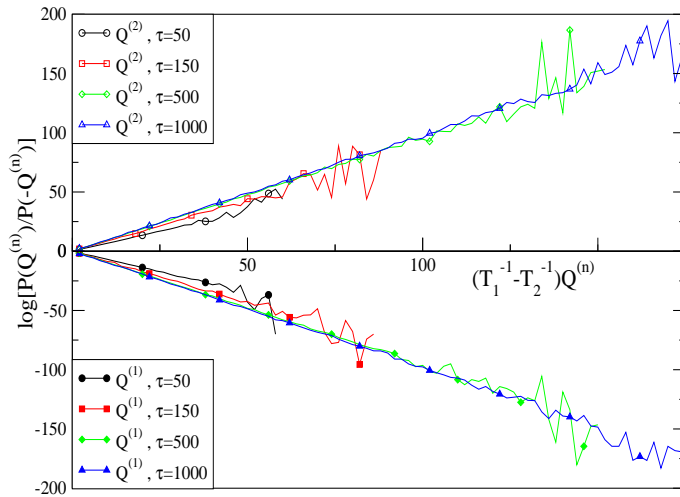


Figure 2. Same parameters of Fig. 1. $\log [P(Q^{(n)}(\tau))/P(-Q^{(n)}(\tau))]$ is plotted against $(1/T_1 - 1/T_2)Q^{(n)}(\tau)$ ($n = 1$ lower panel, $n = 2$ upper panel).

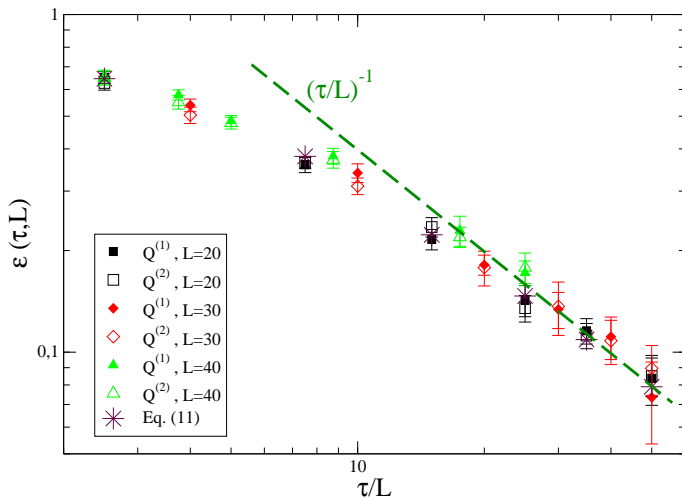


Figure 3. Same parameters of Fig. 1 (different sizes). $\epsilon(\tau, L)$ is plotted against τ/L for different L . Results from a fit based on formula (14) are also shown.

The only characteristic time above T_c is the (microscopic) relaxation time that can be measured from the decay of the autocorrelation function; it is of few MCS for the case of Fig. 1. At sufficiently large τ , greater than the relaxation time, due to the central limit theorem, one expects a Gaussian behavior for the probability distributions, namely $\mathcal{P}(\mathcal{Q}^{(n)}(\tau)) = (2\pi(\sigma_\tau^{(n)})^2)^{-1/2} \exp[-\frac{(\mathcal{Q}^{(n)}(\tau) - \langle \mathcal{Q}^{(n)}(\tau) \rangle)^2}{2(\sigma_\tau^{(n)})^2}]$, with $\langle \mathcal{Q}_\tau^{(n)} \rangle \sim \tau$ and $\sigma_\tau^{(n)} \sim \sqrt{\tau}$. This form is found with good accuracy, as shown by the collapse of the PD's at different times in the inset of Fig. 1.

In Fig. 2, in order to study the FR (2), the logarithm of the ratio $\mathcal{P}(\mathcal{Q}^{(n)}(\tau))/\mathcal{P}(-\mathcal{Q}^{(n)}(\tau))$ is plotted as a function of $\Delta\beta^{(2)}\mathcal{Q}^{(n)}(\tau)$. For every value of τ the data are well consistent with a linear relationship even if, for large values of the heat, the statistics becomes poor. The FR (2) is verified if the slopes

$$D^{(n)}(\tau) = \frac{\ln \frac{\mathcal{P}(\mathcal{Q}^{(n)}(\tau))}{\mathcal{P}(-\mathcal{Q}^{(n)}(\tau))}}{\mathcal{Q}^{(n)}(\tau)\Delta\beta^{(n)}} \quad (8)$$

tend to 1 when $\tau \rightarrow \infty$. In Fig. 3 the behavior of the *distance* $\epsilon^{(n)} = 1 - D^{(n)}(\tau)$ from the expected asymptotic result is shown for the case of Fig. 1. Indeed, this quantity goes to zero for large τ showing the validity of Eq. (2).

A similar behavior occurs in the case with dynamic couplings. In the upper panel of Fig. 4 the PD's for the interface and bulk exchanged heats $\mathcal{Q}^{(2)}$ and $\mathcal{Q}^{(1)}$ are shown. The PD's corresponding to the colder bath are always higher and narrower. As in the case with static coupling, also now the PD's at different τ can be rescaled on a single Gaussian master curve, as it can be seen in the inset of the upper panel of Fig. 4. The distances $\epsilon^{(n)}$ tend to zero, as shown in Fig. 5, and the fluctuation relation (2) is verified. A scaling argument predicting the behavior of $\epsilon^{(n)}$ will be presented in Sec. 2.4.

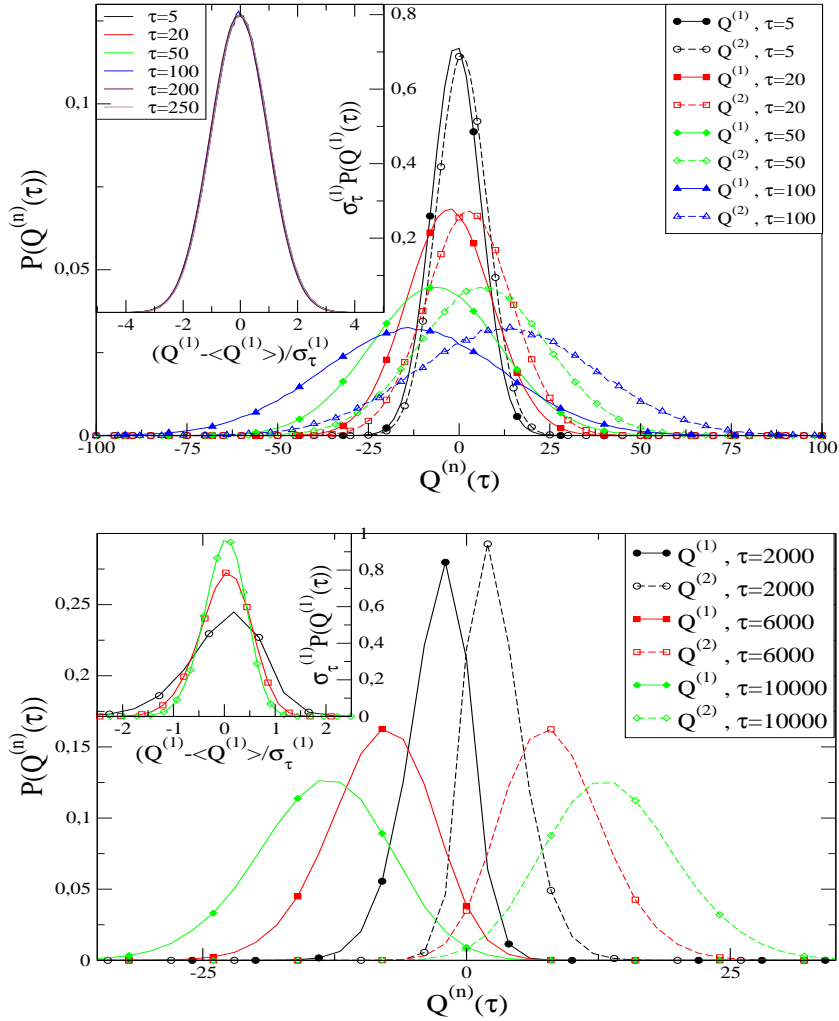


Figure 4. Upper panel ($T_1, T_2 > T_c$): Heat PDs for bulk heat $Q^{(1)}$ (on the left) and interface heat $Q^{(2)}$ (on the right) for the system with dynamical coupling and $T_1 = 3.0, T_2 = 3.1$, size 10×10 and $t_F = 5 \cdot 10^8$ MCS. In the inset $\sigma_\tau^{(1)} \mathcal{P}(Q^{(1)}(\tau))$ is plotted against $(Q^{(1)}(\tau) - \langle Q^{(1)}(\tau) \rangle) / \sigma_\tau^{(1)}$. Curves for different τ collapse on a Gaussian mastercurve. Lower panel ($T_1, T_2 < T_c$): Same kind of plot for $T_1 = 1, T_2 = 1.3$, size 10×10 and $t_F = 10^9$ MCS. The inset shows that PD's at different τ do not collapse on a single curve after rescaling.

2.3. Deviations from the Green-Kubo relation

As discussed in the introduction, once the validity of the FR has been ascertained in this context, it is interesting to see if deviations from the Green-Kubo relation are observed, in order to provide a rigid test of the FR not related to linear response theory. The GKR for the current $\mathcal{J} = | \langle Q^{(n)}(\tau) \rangle | / \tau$ (which does not depend on n due to Eq. (7)) reads

$$\lim_{\Delta T \rightarrow 0} \frac{\mathcal{J}}{\Delta T} = \frac{\mathcal{D}}{2T_1^2} \quad (9)$$

where \mathcal{D} is related to the fluctuations of the heat \mathcal{Q} exchanged with the bath in the equilibrium state at T_1 through

$$\mathcal{D} = \frac{\langle \mathcal{Q}(\tau)^2 \rangle}{\tau}. \quad (10)$$

In order to check if the GKR (9) is verified we proceeded as follows: i) from an equilibrium simulation at $T_1 = 3$ we have extracted \mathcal{D} and ii) by fixing T_1 and varying ΔT in the range $[0, 1]$ we have computed the current \mathcal{J} . We have used the largest values of τ for which the slope (8) is measurable and the FR was verified.

The data for the case with dynamical coupling to the baths are shown in Fig. 6. Our simulations clearly show deviations from the GKR (9) in a range of τ where the FR holds. The same conclusion is arrived at in the case with static coupling to the reservoirs. This proves that in the cases considered insofar the FR is verified beyond the linear regime.

2.4. Scaling behavior of finite- τ corrections

Generally, $\epsilon^{(n)}$ depend on the temperatures, the geometry of the system and on τ . We propose now a scaling argument for the behavior of this quantity that takes also in account the nature of the coupling with the reservoirs. Considering a trajectory of length τ in configuration space, enforcing Eq. (6), one can compute the ratio between the probability of the trajectory $\mathcal{P}(traj)$, conditioned to a given initial state, and that of the time-reversed evolution, obtaining

$$\frac{\mathcal{P}(traj)}{\mathcal{P}(-traj)} = e^{-\frac{\mathcal{Q}^{(1)}(\tau)}{T_1} - \frac{\mathcal{Q}^{(2)}(\tau)}{T_2}} = e^{\mathcal{Q}^{(n)}(\tau)\Delta\beta^{(n)} - \frac{\Delta E}{T_{n'}}}, \quad (11)$$

where $n' \neq n$ and $\Delta E = \mathcal{Q}^{(1)}(\tau) + \mathcal{Q}^{(2)}(\tau)$ is the difference between the energies of the final and initial states. From Eq. (11), after averaging over all possible trajectories [30], it is straightforward to arrive to the following expression

$$\left\langle \frac{\mathcal{P}^{staz}(\tau)}{\mathcal{P}^{staz}(0)} e^{\frac{\Delta E}{T_{n'}}} \right\rangle = \langle e^{-\epsilon^{(n)}\Delta\beta^{(n')}\mathcal{Q}^{(n)}(\tau)} \rangle, \quad (12)$$

where $\mathcal{P}^{staz}(0)$ ($\mathcal{P}^{staz}(\tau)$) is the probability of the initial (final) state.

In order to proceed further, we make a *quasi equilibrium* hypothesis, namely

$$\frac{\mathcal{P}^{staz}(\tau)}{\mathcal{P}^{staz}(0)} \simeq e^{-\beta_1\Delta E_1 - \beta_2\Delta E_2} \quad (13)$$

with $\Delta E = \Delta E_1 + \Delta E_2$. This is a strong assumption which is not expected to hold true in general. However it should be correct when the non-equilibrium drive is small, and the system is such that the NESS approaches the equilibrium state in the limit of small drive ‡. In the present case, therefore, it is expected to apply for small ΔT ,

‡ The fulfillment of this condition is not obvious, particularly in systems with ergodicity breaking. It is not verified in the low temperature phase of the large-N model under shear flow [31], a model related (but with a *mean field* character) to the Ising one considered in this paper, nor in some driven mean field models, see [32].

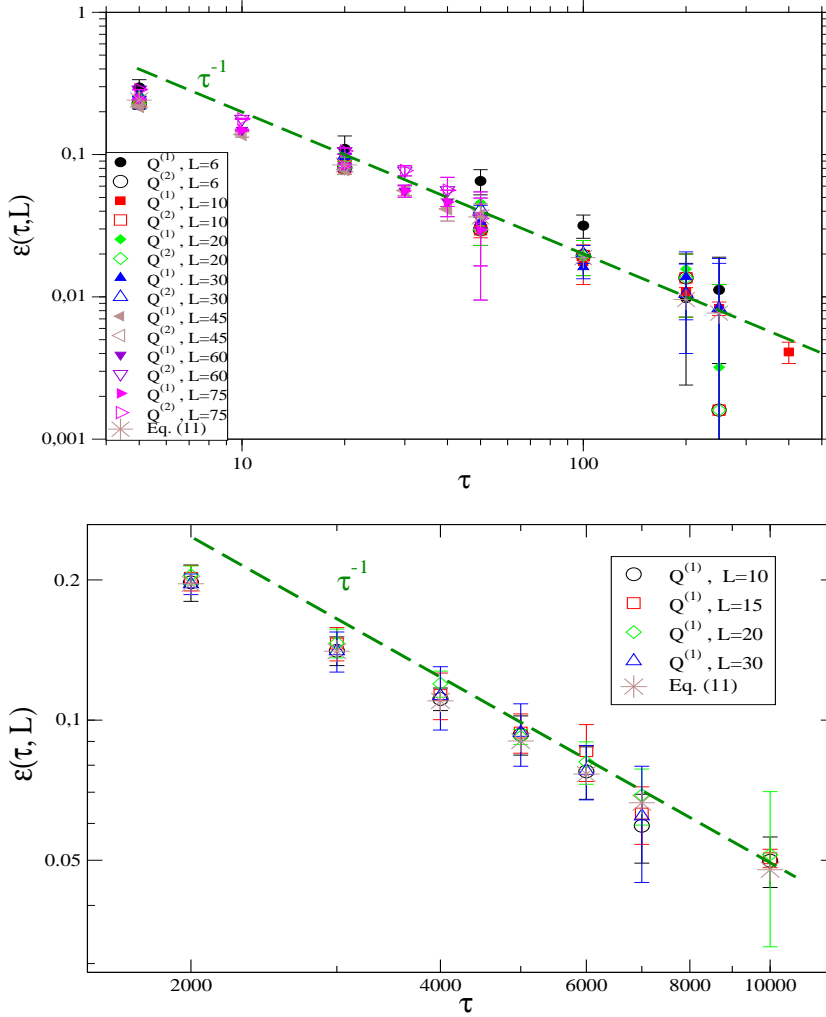


Figure 5. Same parameters of Fig. 4 (different sizes). Upper Panel ($T_1, T_2 > T_c$): $\epsilon^{(n)}(\tau, L)$ are plotted against τ for different L . Lower panel ($T_1, T_2 < T_c$): $\epsilon^{(1)}$ is plotted against τ for different L .

which is indeed the case of our simulations, in the high temperature disordered phase. Furthermore, assuming that ΔE_n and $Q^{(n)}$ are Gaussian distributed (which has been actually verified numerically for $T_1, T_2 > T_c$), one finally arrives at

$$\epsilon^{(n)} \Delta\beta^{(n)} \simeq -\frac{\langle Q^{(n)}(\tau) \rangle}{(\sigma_\tau^{(n)})^2} \mp \sqrt{\left(\frac{\langle Q^{(n)}(\tau) \rangle}{(\sigma_\tau^{(n)})^2} \right)^2 + \frac{v_{\Delta E}^2}{(\sigma_\tau^{(n)})^2} (\Delta\beta^{(n)})^2} \quad (14)$$

where the signs $-$, $+$ are for $n = 1, 2$, respectively, and $v_{\Delta E}^2$ is a quantity related to the variance of ΔE_n which, for large τ , is expected not to depend much on τ .

As discussed above, for large τ , the quantities $\langle Q^{(n)}(\tau) \rangle$ and $(\sigma_\tau^{(n)})^2$ grow proportionally to τ , so that their ratio is asymptotically constant. More precisely, since the heat is exchanged between neighboring spins coupled to different reservoirs,

indicating by N_{flux} the number of such couples of spins we expect $\mathcal{Q}^{(n)}(\tau) \propto (\sigma_\tau^{(n)})^2 \propto N_{flux}\tau$. In the model with static coupling to the baths one has $N_{flux} \propto L$. With dynamic coupling, instead, since every spin in the system can feel one or the other temperature, one has $N_{flux} \propto N$. Since $v_{\Delta E}^2$ is an extensive quantity proportional to the number N of spins, from Eq. (14) one obtains the scaling form $\epsilon^{(n)}(\tau, L) \simeq f(x)$, with

$$x = \begin{cases} \tau L^{-1} & \text{static coupling to baths} \\ \tau & \text{dynamic coupling to baths} \end{cases} \quad (15)$$

and $f(x)$ is a (temperature dependent) scaling function with the large- x behavior $f(x) \sim x^{-1}$. Notice that the corrections to the universal law (2) are system dependent but with the same asymptotic dependence on τ . We will now examine the validity of this scaling behavior in the cases considered so far.

For the system with static coupling the data of Fig. 3 confirm our predictions: Curves with different L collapse when plotted against $x = \tau/L$, for all the values of x considered, and $\epsilon^{(n)} \propto x^{-1}$ for sufficiently large τ . We reported also the results obtained by applying formula (14) with $v_{\Delta E}^2$ used as a fitting parameter; we observe a very good overlap with the numerical data. As expected, the fitting parameter results to be a quantity proportional to the total number N of lattice sites. Moreover, we considered different cases by varying $\Delta\beta$ in the interval 0.1-0.4 at fixed T_1 , and we did not find a significant dependence of the fitting parameter on $\Delta\beta$.

The forms (14) and (15) are also verified for the Ising model with dynamical coupling (see Fig. 5). Sizes between $L = 6$ and $L = 75$ have been considered. The data collapse when plotted as a function of τ (except, perhaps, for the system of size $L = 6$ which is probably too small for our scaling argument to fully apply). At large τ one observes $\epsilon^{(n)} \sim \tau^{-1}$, while preasymptotic results are again well reproduced by Eq. (14).

2.5. Results for $T_1, T_2 < T_c$

Before discussing the results of the simulations in the low temperature phase it is useful to overview the behavior of the Ising model in contact with a single bath at temperature $T < T_c$. In the thermodynamic limit the system is confined into one of the two pure states, which can be distinguished by the sign of the magnetization $m(T) = (1/N) \sum_{i=1}^N \sigma_i$. This state is characterized by a finite relaxation time $\tau_{eq}(T)$. When N is finite, instead, genuine ergodicity breaking does not occur. Nevertheless, the system remains trapped into the basin of attraction of the pure states also in this case, although only for a finite time $\tau_{erg}(N, T)$. Therefore, for a finite size system in the low temperature phase, there is the additional timescale $\tau_{erg}(N, T)$, beside $\tau_{eq}(T)$, which can grow large. This ergodic time diverges when $N \rightarrow \infty$ or $T \rightarrow 0$, when $\tau_{eq}(T)$ is left as the only time scale in the system. For what follows, it is important to recall that, due to the trapping discussed above, an observation of a finite system on timescales much smaller than $\tau_{erg}(N, T)$ is representative of the state with ergodicity breaking which, however, strictly speaking, can be only realized for $N = \infty$.

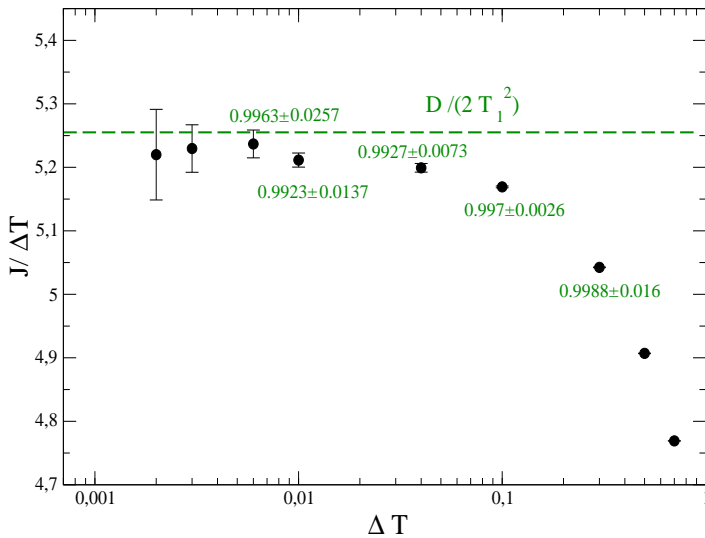


Figure 6. The quantity $\mathcal{J}/\Delta T$ is plotted against ΔT for the system with dynamic coupling to the baths, size 10×10 , $T_1 = 3$. The horizontal dashed line is the value of $\mathcal{D}/(2T_1^2)$ obtained from the simulation of the system in the equilibrium state at T_1 . Near some of the points the values of the slopes $D^{(1)}(\tau)$ at $\tau = 450$ have been reported.

A similar picture holds for systems in contact with two thermal baths, where there are two *ergodic times* $\tau_{erg}(N, T_n)$, one for each subsystem. Since the FR is expected to hold for τ larger than the typical timescales of the system, it is interesting to study the role of the additional timescales $\tau_{erg}(N, T_n)$ on the FR and the interplay between τ and $\tau_{erg}(N, T_n)$.

We have studied numerically the model with dynamic coupling to the baths at $T_1, T_2 < T_c$. $\tau_{erg}(N, T_n)$ can be evaluated as the time over which the autocorrelation functions $C^{(n)}(t - t') = \langle \sum_{i=1}^N \sigma_i^{(n)}(t) \sigma_i^{(n)}(t') \rangle$, where $\sigma_i^{(n)}$ denote spins in contact with the bath at $T = T_n$, decay to zero (notice that $\tau_{erg}(N, T_1) > \tau_{erg}(N, T_2)$ since $T_1 < T_2$). Then, by varying T_1, T_2 and N appropriately one can realize the limit of large τ in the two cases with i) $\tau \ll \tau_{erg}(N, T_2)$ or ii) $\tau \gg \tau_{erg}(N, T_1)$. In the former case, in the observation time-window τ the system is practically confined into pure states while in the latter ergodicity is restored. Not surprisingly, in the latter case, we have observed a behavior very similar to that with $T_1, T_2 > T_c$, except for the timescales required to access the asymptotic stage which are much larger in the low temperature regime, due to the tiny amount of heats exchanged. In particular, the PDs are found to be Gaussian. More interesting is the case i), for which the PDs are shown in the lower panel of Fig. 4. The distributions extend on a smaller support, compared with those for $T_1, T_2 > T_c$, even if the times over which the heats $\mathcal{Q}^{(n)}$ are collected are larger (see insets of the upper panel of Fig. 4). Moreover, quite interestingly, in this case the PDs

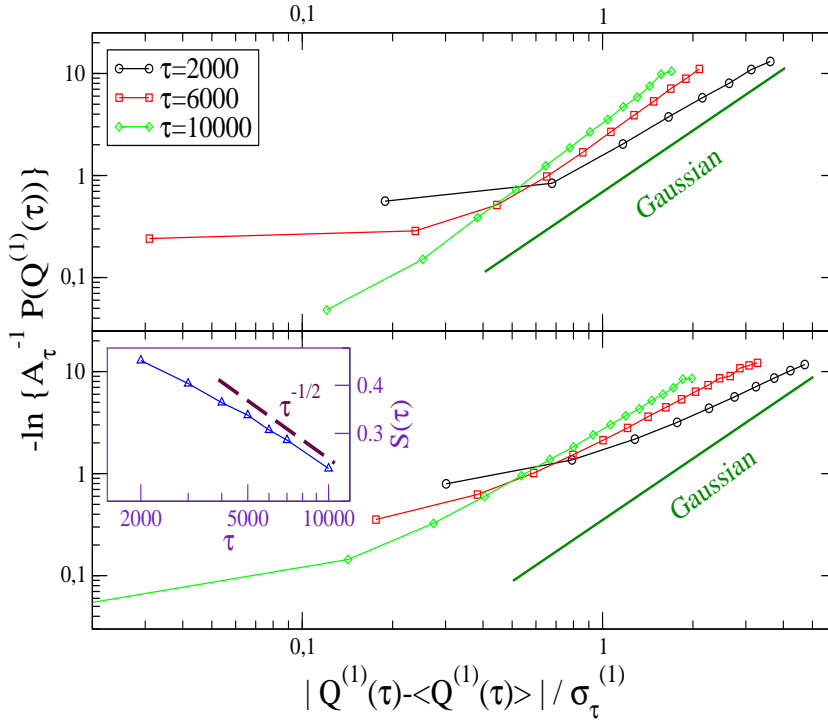


Figure 7. The logarithm of the PDs of the lower panel of Fig. 4 (for $Q^{(1)}$ only) (normalized by the height of A_τ of the peak) is plotted against $|Q^{(1)}(\tau) - \langle Q^{(1)}(\tau) \rangle| / \sigma_\tau$. In the upper (lower) panel the branch $Q^{(1)} < \langle Q^{(1)} \rangle$ ($Q^{(1)} > \langle Q^{(1)} \rangle$) is plotted. The continuous line is the Gaussian behavior. In the inset the skewness is plotted against time. The dashed line is the power law behavior $\tau^{-1/2}$.

are not Gaussian in the range of times accessed by the simulations. This can already be seen from the lower panel of Fig. 4, since the PDs are not symmetric with respect to the maximum. In particular, the right (left) tail of the distribution of $Q^{(2)}$ ($Q^{(1)}$) is visible fatter than the left (right) one. As a further test, in the inset of the same figure we tried to collapse the curves similarly to what done in the upper panel for the case above T_c , but, due to the non Gaussian behavior, the collapse fails. In order to study the shape of the PDs more carefully, in Fig. 7 we plot the logarithm of the PD for $Q^{(1)}$ (normalized by the height of A_τ of the peak) against $|Q^{(1)}(\tau) - \langle Q^{(1)}(\tau) \rangle| / \sigma_\tau$, where σ_τ^2 is the variance of the distribution proportional to τ . In this representation, a Gaussian PD should correspond to a power law, namely a straight line of slope 2. The figure shows that the Gaussian behavior is approached as τ increases. For finite τ , however, the distribution is strongly non Gaussian both around the average $Q^{(1)} \simeq \langle Q^{(1)} \rangle$ and on the tails. In particular, the slope of the *positive* tail with $Q^{(1)} \gg \langle Q^{(1)} \rangle$ (lower panel) is always smaller than that of the *negative* one, confirming that the former is fatter. In addition, the approach to a Gaussian behavior is faster for the negative tail. This pattern of behavior can be expressed quantitatively by the skewness $S(\tau) = \langle (Q(\tau) - \langle Q(\tau) \rangle)^3 \rangle / \langle (Q(\tau) - \langle Q(\tau) \rangle)^2 \rangle^{3/2}$ of the distributions. This quantity is plotted in the inset of Fig. 7, showing a power law decay consistent with $S(\tau) \sim \tau^{-a}$, with $a \simeq 1/2$.

Regarding the slopes $D^{(n)}(\tau)$, they converge to 1 and the scaling $\epsilon(\tau, L) \sim 1/x$ with $x = \tau$ is verified, as shown in Fig. 5 (we have not reported the data for $\mathcal{Q}^{(2)}$ which are more noisy than those for $\mathcal{Q}^{(1)}$). We observe that a fit based on Eq. (14) well reproduces the simulation data also in this case. As anticipated, the times required to reach the slope 1 are much longer than the corresponding ones at high temperature (but always smaller than $\tau_{erg}(N, T_2) \gtrsim 5 \times 10^8$ MCS). These results suggest that the FR (2) and the scalings (14,15) hold even in states with symmetry breaking and that the presence of the macroscopic timescales $\tau_{erg}(N, T_n)$ do not affect their validity. Recalling the discussion at the beginning of this section, it is reasonable to conjecture that for $\tau \ll \tau_{erg}(N, T_2)$ the system enters a NESS which is representative of the state with broken symmetry that one would have (indefinitely) for an infinite system. For the same mechanism discussed above in equilibrium conditions, in this state there is a single relaxation time left (playing the role of $\tau_{eq}(T)$), and the FR is obeyed on timescales larger than this microscopic time. Moreover, recalling the discussion of Sec. 1, this case is particularly interesting since the FR is verified (although with the preasymptotic corrections described by Eq. (14)) in a far from equilibrium situation in which the PDs are not Gaussian.

3. Stationary states under shear

In the present section we consider a system which is coupled to a single heat bath and is mechanically driven out of equilibrium. Mechanical work is done on the system by shearing it in the horizontal direction. Boundary conditions are periodic in the horizontal direction (parallel to the shear) and open in the vertical direction. In a shear event, the horizontal line with coordinate $y \in \{1, \dots, L\}$ is moved by λy lattice steps to the right. Shear events occur at regular intervals of r elementary Monte Carlo moves, with the shear period r submultiple of $N = M \times L$. For each Monte Carlo sweep (MCS) over the lattice there are $N/2$ Kawasaki moves and N/r shear events. This model can be thought of as a discrete version for the kinetic equation of a binary mixture subject to the convective velocity $v_x(y) = \lambda y/(r/N)$ having a shear rate $\dot{\gamma} = \frac{dv_x}{dy} = \lambda N/r$. The model, with single-spin-flip dynamics, was used to study domain growth properties of sheared systems in [33].

The heat released to the bath during the evolution will be computed as in Eq. (5), where the index (n) will be dropped since here the system is exchanging energy with a single reservoir at temperature T . Work done on the system is instead defined as the energy variation in shear events.

Starting from a random configuration, with shear applied at a constant rate, a steady state is reached. As before, the PDs for heat and work relative to the steady state can be constructed collecting the values integrated over segments of length τ in a long trajectory.

In the following we report results obtained for a 50×4 lattice, with $T = 5$, shear step $\lambda = 1$ and shear period $r = 50$, which corresponds to a shear rate $\dot{\gamma} = 4$. Data have been taken mainly with 10^7 MCS to reach the NESS and 10^8 MCS for the measurements.

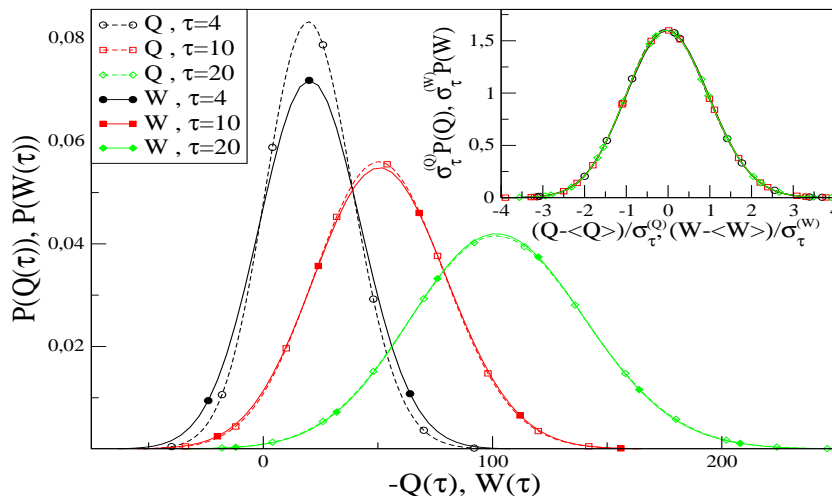


Figure 8. Heat and work PDs for the system under shear at different τ . $5 \cdot 10^7$ MCS have been discarded in order to reach stationarity and $5 \cdot 10^8$ MCS have been used for measurements. See text for the other parameters. In the inset the curves are separately rescaled as in Fig. 1 ($\sigma_\tau^{(Q)}$ and $\sigma_\tau^{(W)}$ are the standard deviations of Q and W , respectively, for different τ).

A few longer ($5 \cdot 10^8$ MCS) runs have been made for some data points.

In Fig. 8 we show the work and heat PDs. At smaller τ the heat distributions are more peaked than the work PDs while they become more similar when τ increases. In all cases the PDs are very well fitted by Gaussian distributions and the work and heat PDs at different τ collapse on a master curve when rescaled as in Fig. 1.

As in Sect. 2, also here we define the distance from the expected asymptotic behavior $\epsilon^{(\mathcal{O})} = 1 - D^{(\mathcal{O})}(\tau)$ where, analogously to Eq. (8), the slope $D^{(\mathcal{O})}(\tau)$ is defined as

$$D^{(\mathcal{O})}(\tau) = \pm \frac{\ln(\mathcal{P}(\mathcal{O}(\tau))/\mathcal{P}(-\mathcal{O}(\tau)))}{\mathcal{O}(\tau)/T} \quad (16)$$

where the signs $+, -$ are for $\mathcal{O} = W, Q$, respectively. In Fig. 9 we report the behavior of $\epsilon^{(\mathcal{O})}$ as a function of τ . $\epsilon^{(\mathcal{O})}$ tend to zero, but differently than in the case of thermodynamic driving, the approach to the expected asymptotic result is slower, especially for the heat.

Analogously to the case of two thermostats, the ratio of the probability of a trajectory over that of the time-reversed is given by

$$\frac{\mathcal{P}(\text{traj})}{\mathcal{P}(-\text{traj})} = e^{-\frac{Q(\tau)}{T}} = e^{\frac{W(\tau)}{T} - \frac{\Delta E}{T}}, \quad (17)$$

where, for each trajectory, the relation $Q(\tau) + W(\tau) = \Delta E$ holds. Proceeding as in the case with thermodynamic drive one arrives at an expression similar to Eq. (14)

$$\epsilon^{(\mathcal{O})} = \mp \frac{T \langle \mathcal{O}(\tau) \rangle}{(\sigma_\tau^{(\mathcal{O})})^2} + T \sqrt{\left(\frac{\langle \mathcal{O}(\tau) \rangle}{(\sigma_\tau^{(\mathcal{O})})^2} \right)^2 + \frac{v^2}{(\sigma_\tau^{(\mathcal{O})})^2}}, \quad (18)$$

where the signs $-, +$ are for W, Q respectively, and v^2 is an unknown quantity that can be used as a fit parameter. In doing that we find a very good agreement between

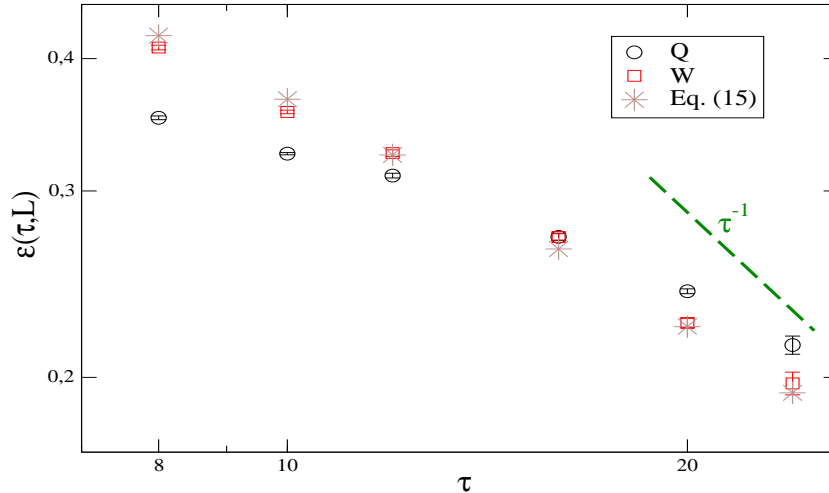


Figure 9. $\epsilon^{(\mathcal{O})}$ ($\mathcal{O} = Q, W$) as a function of τ for the same system of Fig. 8.

formula (18) and the numerical data for W , while the accordance (not shown in Fig. 9) is very poor for Q , probably because, as already noticed, this quantity has a slower convergence. The faster convergence of W can be possibly ascribed to the fact that, after making the quasi-equilibrium assumption $\frac{\mathcal{P}^{staz}(\tau)}{\mathcal{P}^{staz}(0)} \simeq e^{-\beta\Delta E}$ and calculating the averages over trajectories as in Sec. 2.4, the boundary term proportional to ΔE cancels for the work while it remains when one consider the behavior of the heat.

4. Discussion and Conclusions

In this Article we have considered the issue of the FRs in the Ising model with nearest neighbor interactions. We focused on two different NESS, induced by a thermodynamic drive provided by two thermostats at different temperatures, or by a mechanical forcing realized by shearing the system. We find that the FR (1) is verified in any case when τ is sufficiently large. For the case with different thermostats, we have also provided an exacting test of the FR in the far from equilibrium regime where deviations from the linear response theory are observed with the Green-Kubo relation violated (above T_c), or the PDs are not Gaussian (below T_c). Furthermore, we have analyzed the effects of finite time by proposing a scaling law which takes into account the geometry of the system and the details of the interaction with the baths and that is well verified numerically. According to this law the leading corrections to the FR (1) decay as τ^{-1} , in agreement with what found in some previous studies [3, 11, 17], while the dependence on the system size relies on the details of the coupling to the baths. The derivation of our scaling law is based on few strong but general hypotheses, which could, in principle, be verified also in different systems. A natural perspective for future work, therefore, is the understanding of the possible generality of our results in different contexts.

Most of the results of this paper are obtained for systems that are able to equilibrate in the small entropy production limit [32]. Basically this means that, for this class of systems, the equilibrium state is recovered in a finite time when the drive is switched off.

In this case the FR generally holds, as we have explicitly verified. The generalization of the FR to systems which do not equilibrate in the small entropy production limit is a very interesting issue. Non-equilibration typically happens when the limit of large τ is taken after the thermodynamic limit in systems, such as glasses or ferromagnets below the critical temperature, whose equilibration time diverges with the system size. Regarding these non-equilibrating systems, some conjectures have recently appeared in the literature [34], inferring that a relation similar to (1) holds, where, however, the entropy production, instead of being a function of the bath(s) temperature (as for instance in Eqs.(2,3)), depends on T_{eff} , namely the effective temperature [35] which characterizes the dynamics of these systems. For the model considered in this paper one has $T_{eff} = \infty$ [36]. In this perspective, therefore, it would be very interesting to study the technically demanding case of the Ising model with shear for $T < T_c$.

Acknowledgments

The authors are grateful to G. Saracco and L. Rondoni for useful discussions.

References

- [1] Evans D J, Cohen E G D and Morriss G P, 1993 *Phys. Rev. Lett.* **71** 2401
- [2] Evans D J and Searles D J, 1994 *Phys. Rev. E* **50** 1645
- [3] Gallavotti G and Cohen E G D, 1995 *J. Stat. Phys.* **80** 931; 1995 *Phys. Rev. Lett.* **74** 2694
- [4] Kurchan J, 1998 *J. Phys. A* **31** 3719
- [5] Lebowitz J L and Spohn H, 1999 *J. Stat. Phys.* **95** 333
- [6] Maes C, 1999 *J. Stat. Phys.* **95** 367
- [7] Jarzynski C, 1997 *Phys. Rev. Lett.* **78** 2690
- [8] Crooks G E, 1999 *Ph.D. Thesis* (University of California , Berkeley); 1999 *Phys. Rev. E* **60** 2721
- [9] Hatano T and Sasa S, 2001 *Phys. Rev. Lett.* **86** 3463
- [10] van Zon R and Cohen E G D, 2003 *Phys. Rev. Lett.* **91** 110601
- [11] van Zon R, Ciliberto S and Cohen E G D, 2004 *Phys. Rev. Lett.* **92** 130601
- [12] Seifert U, 2005 *Phys. Rev. Lett.* **95** 040602
- [13] Chetrite R and Gawędzki K, 2007 arXiv:0707.2725
- [14] See e.g. Harris R J and Schütz G M, 2007 *J. Stat. Mech.* P07020; Gallavotti G, arXiv:0711.2755; Ritort F, to appear in *Adv. in Chem. Phys.*; Rondoni L and Mejia-Monasterio C, 2007 *Nonlinearity* **20** R1; Zamponi F, 2007 *J. Stat. Mech.* P02008
- [15] Bustamante C, Liphardt J and Ritort F, 2005 *Phys. Today* **58** 43
- [16] Wang G M, Sevick E M, Mittag E, Searles D J and Evans D J, 2002 *Phys. Rev. Lett.* **89** 050601
- [17] Garnier N and Ciliberto S, 2005 *Phys. Rev. E* **71** 060101
- [18] Douarche F, Joubaud S, Garnier N B, Petrosyan A and Ciliberto S, 2006 *Phys. Rev. Lett.* **97** 140603
- [19] Lepri S, Livi R and Politi A, 1998 *Physica D* **119** 140
- [20] Visco P, 2006 *J. Stat. Mech.* P06006
- [21] Jarzynski C and Wójcik D K, 2004 *Phys. Rev. Lett.* 230602
- [22] Lecomte V, Racz Z and van Wijland F, 2005 *J. Stat. Mech.* P02008
- [23] Chatelain C and Karevski D, 2006 *J. Stat. Mech.* P06005; Híjar H, Quintana-H J and Sutmann G, 2007 *J. Stat. Mech.* P04010
- [24] Piscitelli A, Corberi F and Gonnella G, 2008 cond-mat/arXiv:0807.0392, to appear as Fast Track Comm. of J. of Physics A

- [25] Rondoni L and Morriss G P, 2003 *Open Syst. & Information Dynam.* **10** 105
- [26] Giuliani A, Zamponi F and Gallavotti G, 2005 *J. Stat. Phys.* **119** 909
- [27] Gallavotti G, 1996 *Phys. Rev. Lett.* **77** 4334
- [28] de Oliveira M J, Mendes J F F and Santos M A, 1993 *J. Phys. A* **26** 2317
- [29] Drouffe J M and Godrèche C, 1999 *J. Phys. A* **32** 249; Andrenacci N, Corberi F and Lippiello E, 2006 *Phys. Rev. E* **73** 046124
- [30] Bodineau T and Derrida B, 2007 *C.R. Physique* **8** 540
- [31] Corberi F, Gonnella G, Lippiello E and Zannetti M, 2002 *Europhys. Lett.* **60** 425; Corberi F, Gonnella G, Lippiello E and Zannetti M, 2003 *J. Phys. A* **36** 4729
- [32] Cugliandolo L F, Kurchan J, Le Doussal P and Peliti L, 1997 *Phys. Rev. Lett.* **78** 350; Berthier L, Barrat J L and Kurchan J, 2000 *Phys. Rev. E* **61** 5464; Le Doussal P, Cugliandolo L F and Peliti L, 1997 *Europhys. Lett.* **39** 111
- [33] Cirillo E N M, Gonnella G and Saracco G P, 2005 *Phys. Rev. E* **72** 026139
- [34] Sellitto M, cond-mat/arXiv:9809186; Crisanti A and Ritort F, 2004 *Europhys. Lett.* **66** 253; Zamponi F, Bonetto F, Cugliandolo L F and Kurchan J, 2005 *J. Stat. Mech.* P09013
- [35] Cugliandolo L F, Kurchan J and Peliti L, 1997 *Phys. Rev. E* **55** 3898
- [36] Parisi G, Ricci-Tersenghi F and Ruiz-Lorenzo J J, 1999 *Eur. Phys. J. B* **11** 317; Corberi F, Lippiello E and Zannetti M, 2004 *J. Stat. Mech.* P12007; Cugliandolo L F, cond-mat/arXiv:0210312; Crisanti A and Ritort F, 2003 *J. Phys. A Math. Gen.* **36** R181